AD-A040 746 AIR FORCE GEOPHYSICS LAB HANSCOM AFB MASS F/G 7/2

HIGH RESOLUTION SPECTRA OF CO2 IN THE 3500 TO 3770 CM REGION AT--ETC(U)

FEB 77 H SAKAI, G A VANASSE

UNCLASSIFIED AFGL-TR-77-0039 NL

1 OF 1

ADA040746

END

DATE

FILMED

7 - 77

AD A040746

(12)
B.S.

AFGL-TR-77-0039
ENVIRONMENTAL RESEARCH PAPERS, NO. 592

High Resolution Spectra of CO_2 in the 3500 to 3770 cm^{-1} Region at 625°K

HAJIME SAKAI
GEORGE A. VANASSE

10 February 1977

OPTICAL PHYSICS DIVISION PROJECT 2310

AIR FORCE GEOPHYSICS LABORATORY

HANSCOM AFB, MASSACHUSETTS 01731

AIR FORCE SYSTEMS COMMAND, USAF

This report has been reviewed by the ESD Information Office (OI) and is releasable to the National Technical Information Service (NTIS).

This technical report has been reviewed and is approved for publication.

FOR THE COMMANDER

John Howard

Chief Scientist

Qualified requestors may obtain additional copies from the Defense Documentation Center. All others should apply to the National Technical Information Service.

Unclassified
SECURITY CLASSIFICATION OF THIS PAGE (When Data Entered)

REPORT DOCUMENTATION PAGE		READ INSTRUCTIONS BEFORE COMPLETING FORM
1. REPORT NUMBER AFGL-TR-77-0039, AFGL-ERP-592	2. GOVT ACCESSION NO.	3. RECIPIENT'S CATALOG NUMBER
4. TITLE (and Subtitle) HIGH RESOLUTION SPECTRA OF CO_2 IN THE 3500 TO 3770 cm^{-1} REGION AT 625°K.		5. TYPE OF REPORT & PERIOD COVERED Scientific. Interim
		6. PERFORMING ORG. REPORT NUMBER ERP No. 592
7. AUTHOR(s) Hajime Sakai, George A. Vanasse		8. CONTRACT OR GRANT NUMBER(s)
9. PERFORMING ORGANIZATION NAME AND ADDRESS Air Force Geophysics Laboratory/ OPI Hanscom AFB, Massachusetts 01731		10. PROGRAM ELEMENT, PROJECT, TASK AREA & WORK UNIT NUMBERS 61102F 2310G101 G1
11. CONTROLLING OFFICE NAME AND ADDRESS Air Force Geophysics Laboratory/ OPI Hanscom AFB, Massachusetts 01731		12. REPORT DATE 10 February 1977
		13. NUMBER OF PAGES 28
14. MONITORING AGENCY NAME & ADDRESS(if different from Controlling Office) Environmental research papers,		15. SECURITY CLASS. (of this report) Unclassified
		15a. DECLASSIFICATION/DOWNGRADING SCHEDULE

14 6 10 16 17 11 9 12 26p.

16. DISTRIBUTION STATEMENT (of this Report)

Approved for public release; distribution unlimited.

17. DISTRIBUTION STATEMENT (of the abstract entered in Block 20, if different from Report)

18. SUPPLEMENTARY NOTES

19. KEY WORDS (Continue on reverse side if necessary and identify by block number)

Spectroscopy
Interferometry
CO_2

20. ABSTRACT (Continue on reverse side if necessary and identify by block number)

This report describes results obtained with the Idealab Model 100 interferometer spectrometer of the absorption spectrum of CO_2 at a temperature of 625°K. The hot cell used in the measurements is described in detail and low resolution emission data (2 cm^{-1}) of CO_2 at around 500°K are presented. The absorption spectrum from 3500 to 3770 cm^{-1} of CO_2 at 625°K to a resolution of 0.01 cm^{-1} is presented as well as a simulated spectrum computed using the AFGL line compilation.

DD FORM 1 JAN 73 1473 EDITION OF 1 NOV 65 IS OBSOLETE

Unclassified
SECURITY CLASSIFICATION OF THIS PAGE (When Data Entered)

409 578

1B

Unclassified

SECURITY CLASSIFICATION OF THIS PAGE(When Data Entered)

Unclassified

SECURITY CLASSIFICATION OF THIS PAGE(When Data Entered)

Preface

We wish to acknowledge the contribution of Mr. Ronald Huppi of the Stewart Radiance Laboratory of Utah State University for his cooperation in making the low-resolution CO_2 emission measurements that resulted in Figures 3 and 4.

Contents

Illustrations

Tables

High Resolution Spectra of CO_2 in the 3500 to 3770 cm-1 Region at 625°K

1. INTRODUCTION

The present measurements of CO_2 at an elevated temperature were undertaken in order to update the AFGL line compilation[1] that is used throughout the DoD for determining the spectral characteristics of the atmosphere. Knowledge of the emission, transmission, and absorption of the atmosphere is of crucial importance for military systems that operate either within the atmosphere and/or looking through it. The spectral emission of targets is sometimes due to molecular systems at elevated temperatures, and it is, therefore, necessary to determine their spectral characteristics at these elevated temperatures.

A more fundamental reason for making such measurements is to obtain experimental data to compare with the theoretically predicted spectra. As is the case with CO_2, many times the synthetic spectra are calculated using molecular parameters that were obtained from room-temperature data of lower resolution. It is not surprising that the experimentally obtained high-resolution elevated-temperature data will exhibit differences when compared with the theoretically predicted data. Once the experimental data are obtained, it is possible to recalculate the molecular parameters and also the refined synthetic spectra.

(Received for publication 9 February 1977)

1. McClatchey et al (1973) AFCRL Atmospheric Absorption Line Parameters Compilation, AFCRL-TR-73-0096.

PRECEDING PAGE BLANK-NOT FILMED

Finally, it should be emphasized that knowledge of the spectral characteristics of the atmosphere and of the molecular effluents of military target vehicles (plumes) and stacks is of vital importance for some of the techniques being proposed for military surveillance. These techniques assume certain spectral characteristics for backgrounds and for targets, and operate on the basis of the correlation of the assumed and actual spectral characteristics. Consequently, these techniques depend on the capability of accurately predicting target spectral characteristics; otherwise they are ineffective and have high false-alarm rates.

The 2.7 μ spectral characteristics of CO_2 at 625°K and with a resolution of 0.01 cm^{-1} were obtained in the present measurements and are reported here. The experimental conditions for the measurements are described and the obtained data compared with the theoretically predicted data that forms part of the AFGL line compilation.

2. EXPERIMENTAL TECHNIQUE

The instrument used to obtain the high-resolution data is the Idealab Model 100 interferometer spectrometer (Figure 1). It is a custom-built, 2 meter path difference cat's eye interferometer that operates in the stepping mode rather than the continuous drive mode. This interferometer and the data-recording scheme have been described in previous publications[2,3] and will not be discussed here. The output data from the interferometer have to be Fourier transformed to obtain the spectral information of interest. A detailed description of the technique for processing the interferometer data can be found in the above publications, and will not be touched upon here. Described herein is the hot cell that had to be assembled for the measurements, as well as the auxiliary interface chamber that is being used to couple the hot cell to the 2 meter path difference interferometer.

The hot cell was originally built for another project, but it was never assembled and tested. When it became evident that high-temperature high-resolution measurements were necessary, for the reasons mentioned above, the hot cell was assembled and tested at low resolution before being brought up to the 2 meter path difference interferometer.

2. Pritchard et al (1973) Two-Meter Path Difference Interferometer for Fourier Spectroscopy, AFCRL-TR-73-0223.

3. Sakai, H. (1974) High-Resolution Fourier Spectroscopy, AFCRL-TR-74-0571.

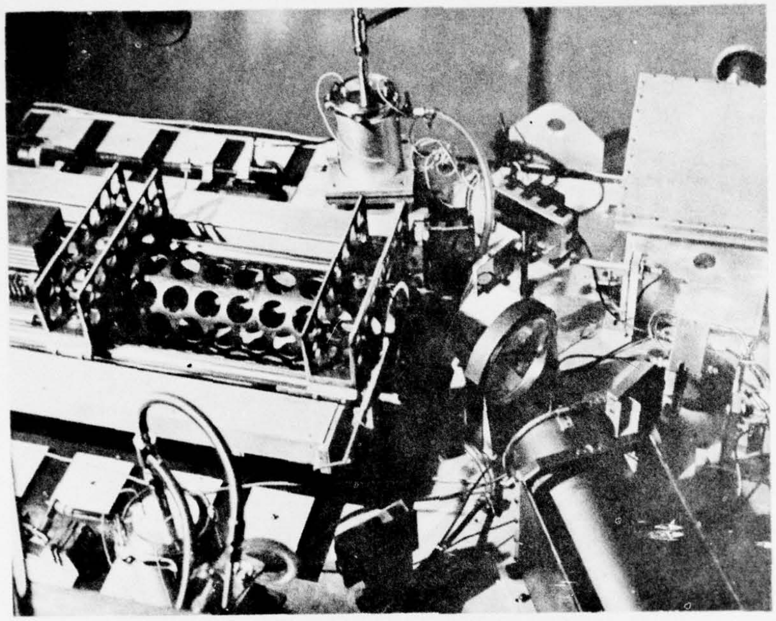

Figure 1. Photograph of Idealab Model 100 Interferometer Spectrometer. The movable cat's eye tube can be seen in center left, the holes in it are to reduce its weight. At the lower right is the fixed cat's eye tube with the beamsplitter slightly above and to the left of it

The hot cell consists of the optical system shown in Figure 2b; Figure 2a shows the optical set-up for the interface chamber that couples the hot cell to the 2 meter path difference interferometer. The hot cell optical system is inside a cylindrical chamber. The volume of gas contained within the optical system is heated by a 65-ft-long heater ribbon that is coiled along a supporting structure surrounding the optical system. This heater ribbon (like a toaster element) essentially forms a cylinder, inside of which is the hot cell optical system. The main cylindrical chamber, which contains this combination of optical system and furnace assembly, has power feed-throughs to heat the cell. Power requirements for this furnace are 240 V at 600 A maximum.

The main chamber has two windows that serve as entrance and exit apertures for the chamber, and are indicated as W in Figure 2b. These windows are sealed with gaskets of silicone rubber and must be cooled by circulating water whenever the cell is to be operated above 200°C. The control unit for the chamber contains an over-temperature protection thermal switch that turns off the furnace when the window temperature gets too high.

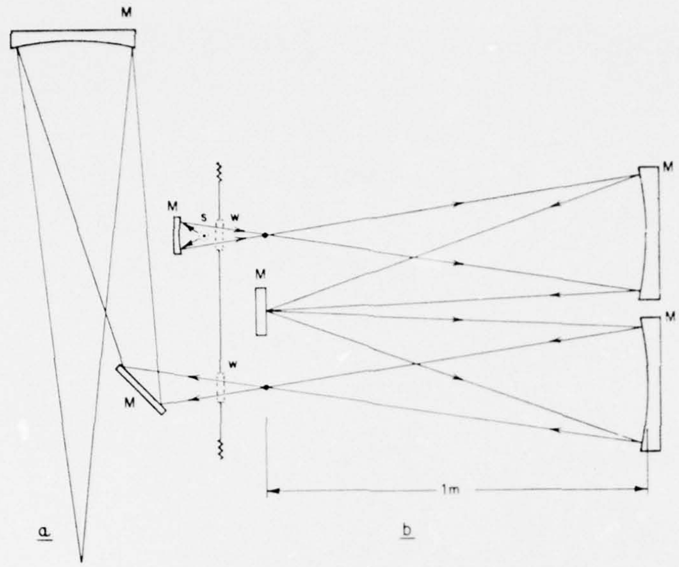

Figure 2. (a) Interface Optical System. Source S is also located in this chamber. (b) Hot Cell Optical System. W's are entrance and exit windows, S is the source, M's are mirrors

The optical cell furnace is designed to operate to temperatures up to 1000°C in an atmosphere of CO_2 at pressures up to about 2 atmospheres absolute. The heater elements and other high-temperature furnace parts are made of molybdenum and alumina with tantalum fasteners. The mirrors inside the cell are made of quartz with a rhodium coating.

The chamber and its doors are water cooled to prevent overheating of the O-ring seals and to maintain outer wall temperatures that are comfortable and safe in case of contact by operating personnel. The O-rings are made of "Viton" and cannot withstand temperatures above 200°C.

The temperature of the hot cell is controlled by a temperature-control system that is designed to have an adjustable set point and a programmable rate of change of temperature. This system controls the output of a power unit that supplies the heating current to the furnace heaters. The current controlling is done according to an error signal, generated by the temperature difference between a thermocouple and the temperature set point, that determines what portion of the 240-V line voltage is to be applied to the heaters. The control unit also has an output current-limiting adjustment to limit the maximum furnace current to 60 A.

The hot cell was assembled and tested to see if it operated as it was supposed to. The temperature of the cell was raised to 950°C and everything seemed to work properly. It was then decided to make low-resolution measurements at an elevated temperature. A small 2 cm^{-1} resolution rapid-scan Michelson interferometer was set up next to the hot cell, the radiation output of which was fed into the interferometer. The cell temperature was stabilized at about 225°C with 0.01 atmosphere of CO_2 pressurized to 0.1 atmosphere with dry N_2. About 100 rapid-scan interferograms were obtained, co-added, and Fourier transformed to obtain the spectra shown in Figures 3 and 4. Figures 3 shows a spectrum of the black-body emission due to the hot cell as well as the CO_2 emission at 4.3 and 2.7 μ.

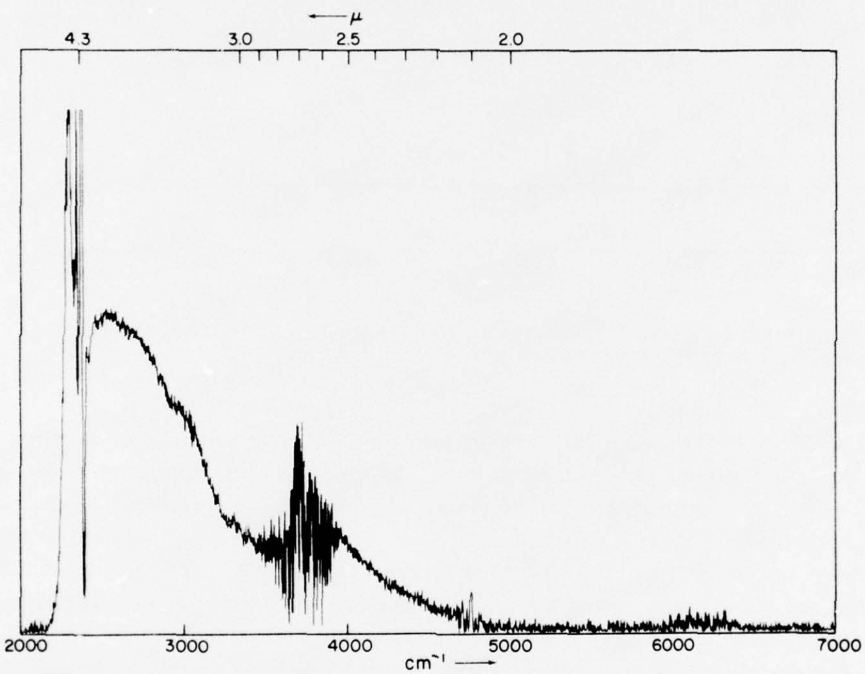

Figure 3. CO_2 Hot Cell Spectrum: Resolution 1.9 cm^{-1}, Gas Temperature 625°K, Raw Spectrum

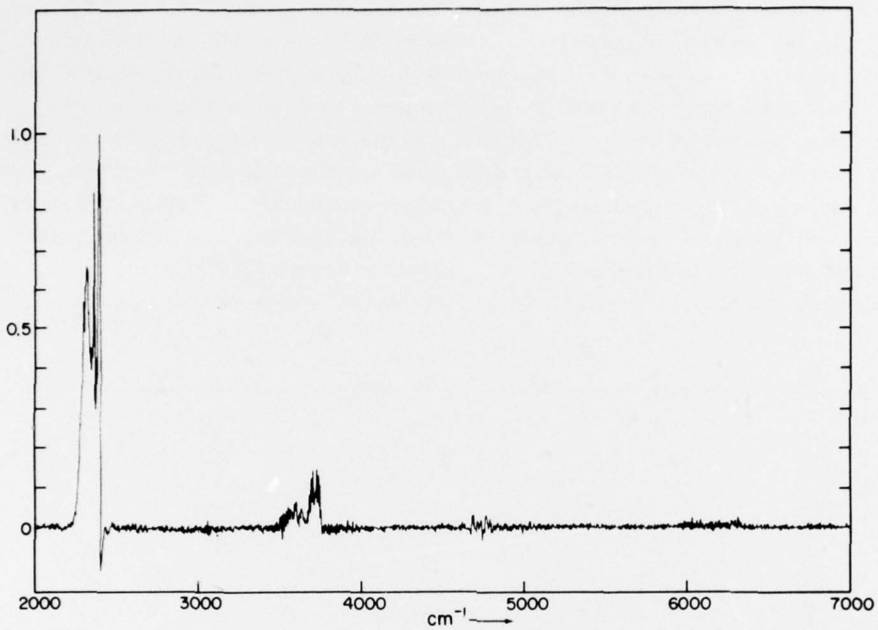

Figure 4. CO_2 Hot Cell Spectrum: Resolution 1.9 cm^{-1}, Gas Temperature 625°K, Background Subtracted

The structure around 2.1 μ has not been identified. (It was noticed that the large blackbody background radiation encumbered the measurement; in trying to come up with means of improving the measurements, a background suppression scheme[4] was conceived.) Figure 4 shows the CO_2 spectrum after the blackbody background radiation had been subtracted from the spectrum of Figure 3. After these measurements, the hot cell was moved near the 2 meter path difference interferometer and coupled to it, using the interface optics illustrated in Figure 2a.

The interface optical system is enclosed in an evacuable chamber that is bolted onto the hot cell chamber. It has an exit aperture window that lies very close to the entrance window or the large chamber containing the 2 meter path difference interferometer. Figure 5 is a photograph of the hot cell and interface chamber in their location abutting the 2 meter path difference interferometer.

4. Vanasse, G.A., Murphy, R., and Cook, F. (1976) Double-beaming technique in Fourier spectroscopy, App. Optics, **15**:290.

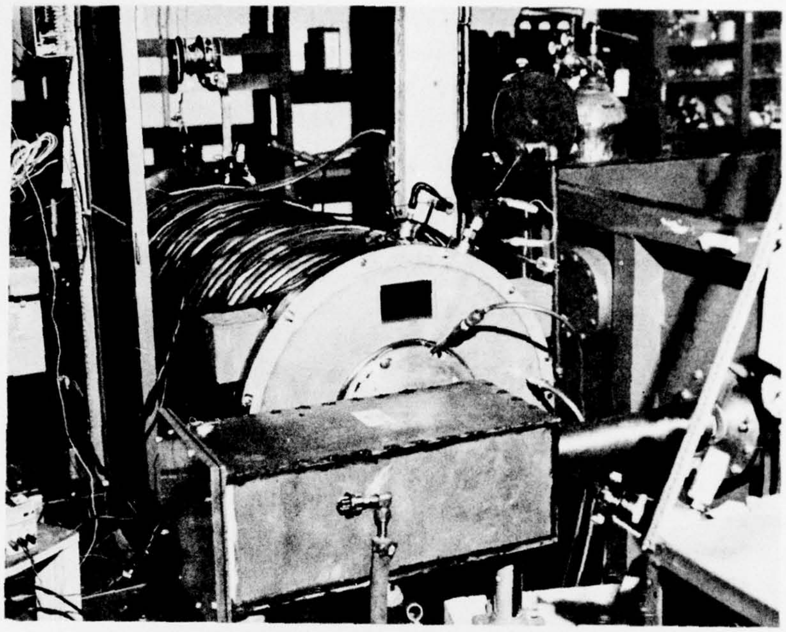

Figure 5. Photograph of Hot Cell and Interface Chamber

3. EXPERIMENTAL DATA AND COMPARISON SPECTRA

The CO_2 spectrum shown in the upper section of Figures 6 through 29 were measured with a pressure of 22.3 mm Hg at a temperature of 625°K and a path length of 4 meters. The spectral resolution was 0.012 cm^{-1}. It was noticed that the spectra obtained were much noisier than those obtained with the same experimental condition at 300°K. The difficulty encountered seemed to originate in the multitraversal cell optics. The positional stability of the optical elements was inadequate for the present measurement, when the cell temperature was operated at an elevated temperature. The spectral data shown were obtained by averaging several interferograms in an attempt to improve the signal-to-noise ratio.

The synthetic spectra shown in the lower trace of Figures 6 through 29 were calculated for a CO_2 pressure of 5.26 mm Hg at 625°K with a spectral resolution of 0.012 cm^{-1}. The lower curves of Figures 6 through 29 are plots of absorptance; that is, the ordinate is a measure of the absorptance. The upper curves, which represent the experimental data, are the absorption spectra.

A definite discrepancy can be detected between these two curves, indicating a need for improvement of the compiled line data. Nonetheless, the bands listed for $C^{12}O_2^{16}$ in Table 1 were identified. A more detailed analysis of these bands will be part of a future study.

Table 1. The Observed $C^{12}O_2^{16}$ Bands and Their Band Centers

Band	Band Center (cm^{-1})
30014 – 20003	3527.703
13312 – 03301	3528.036
21113 – 11102	3542.601
12212 – 02201	3552.841
21112 – 11101	3555.895
30013 – 20002	3556.749
10022 – 00011	3566.063
20013 – 10002	3568.208
22213 – 12202	3578.670
11112 – 01101	3580.334
20012 – 10001	3589.645
10012 – 00001	3612.844
10021 – 00011	3667.544
20012 – 10002	3692.418
21112 – 11102	3700.290
30011 – 20001	3705.927
20011 – 10001	3711.473
21111 – 11101	3713.714
10011 – 00001	3714.781
11111 – 01101	3723.249
12211 – 02201	3726.647
13311 – 03301	3727.380

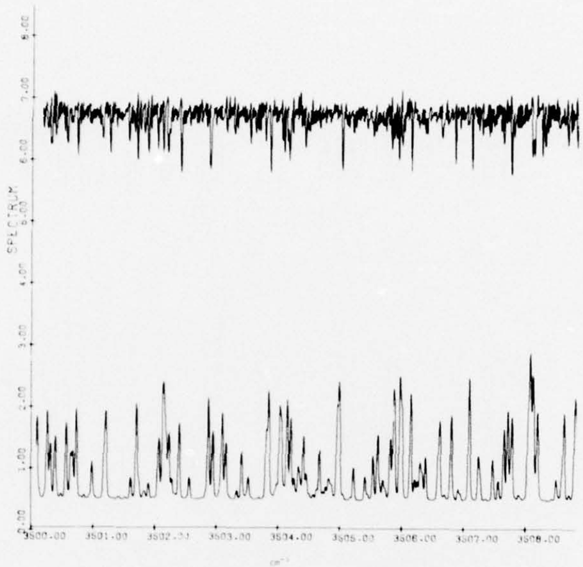

Figure 6. CO_2 Hot Cell Spectrum (upper curve) and Simulated Spectrum (lower curve), 3500 - 3508 cm^{-1}

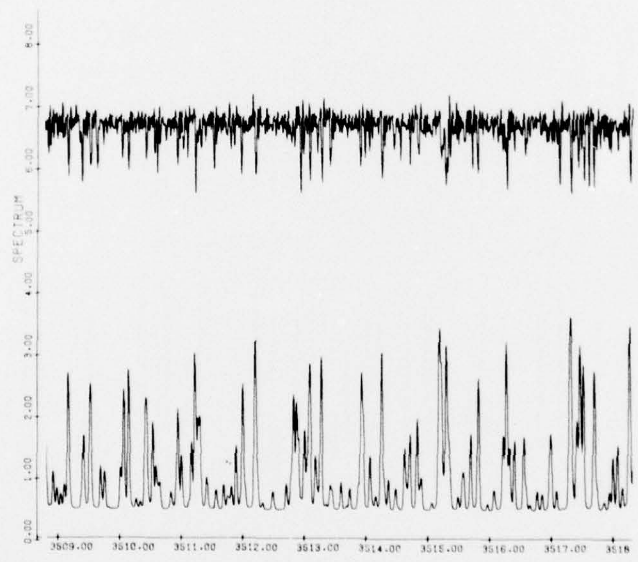

Figure 7. CO_2 Hot Cell Spectrum (upper curve) and Simulated Spectrum (lower curve), 3509 - 3518 cm^{-1}

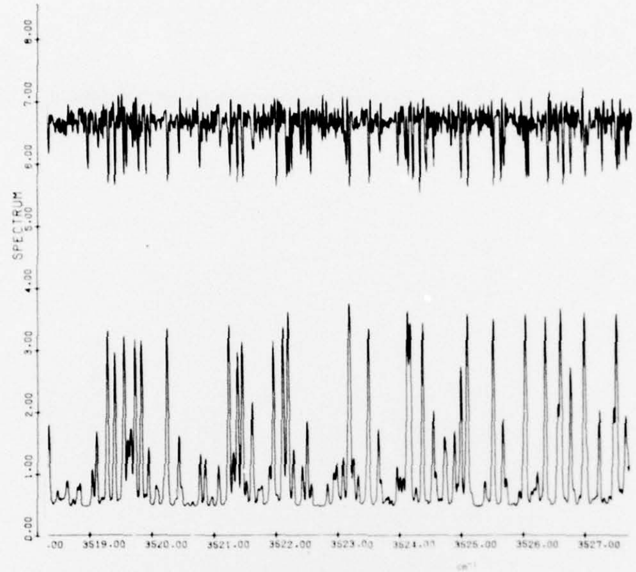

Figure 8. CO_2 Hot Cell Spectrum (upper curve) and Simulated Spectrum (lower curve), 3519 – 3527 cm^{-1}

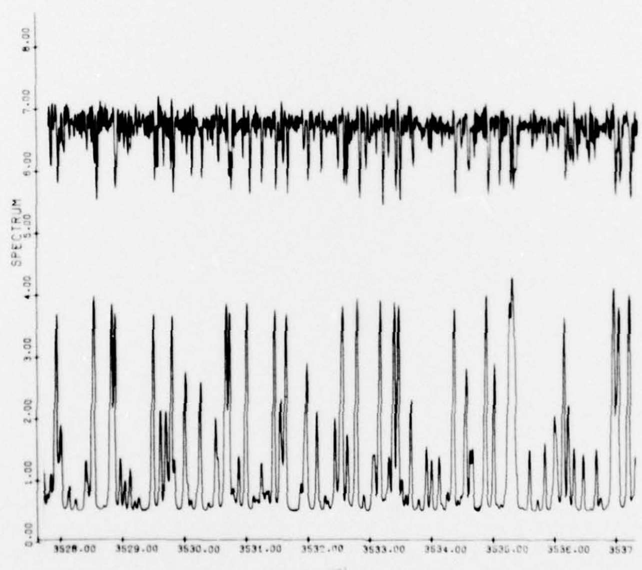

Figure 9. CO_2 Hot Cell Spectrum (upper curve) and Simulated Spectrum (lower curve), 3528 – 3537 cm^{-1}

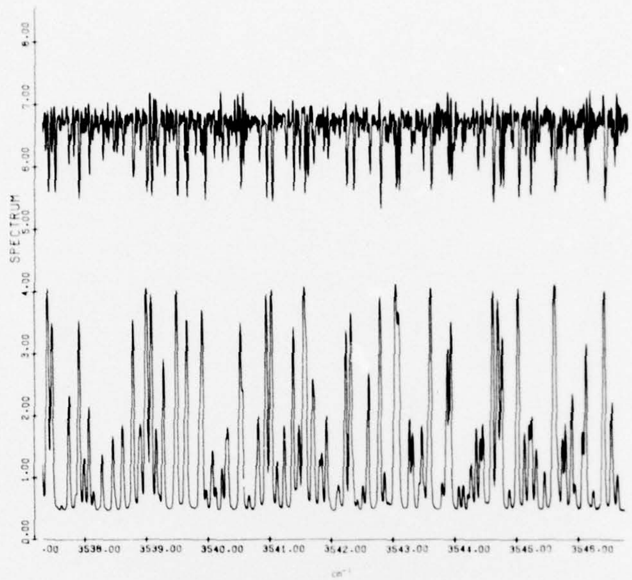

Figure 10. CO_2 Hot Cell Spectrum (upper curve) and Simulated Spectrum (lower curve), 3538 - 3546 cm^{-1}

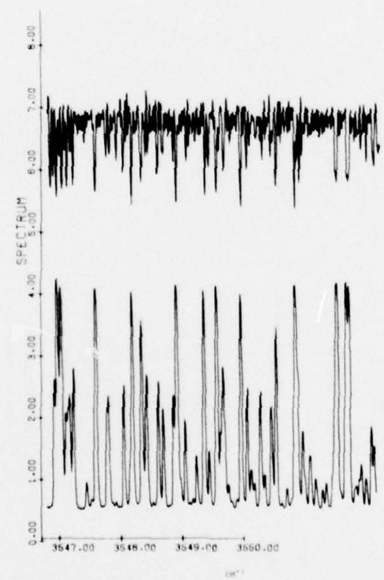

Figure 11. CO_2 Hot Cell Spectrum (upper curve) and Simulated Spectrum (lower curve), 3547 - 3550 cm^{-1}

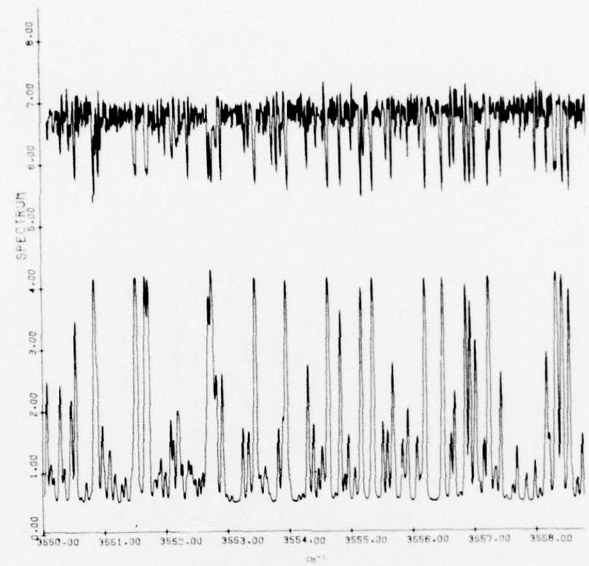

Figure 12. CO_2 Hot Cell Spectrum (upper curve) and Simulated Spectrum (lower curve), 3551 - 3558 cm^{-1}

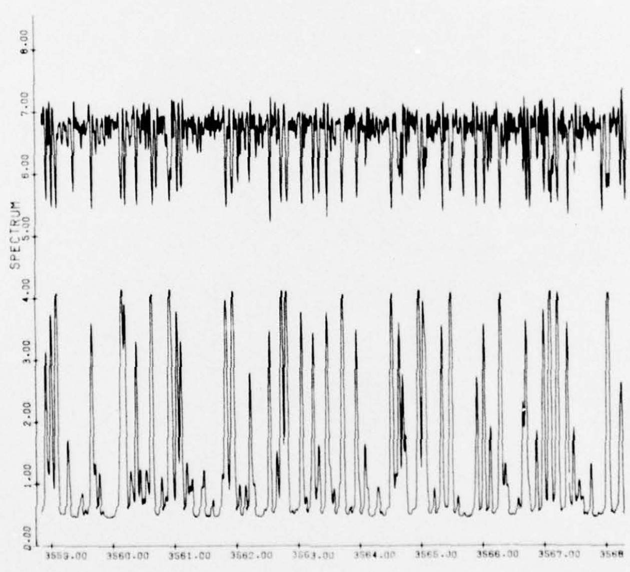

Figure 13. CO_2 Hot Cell Spectrum (upper curve) and Simulated Spectrum (lower curve), 3559 - 3568 cm^{-1}

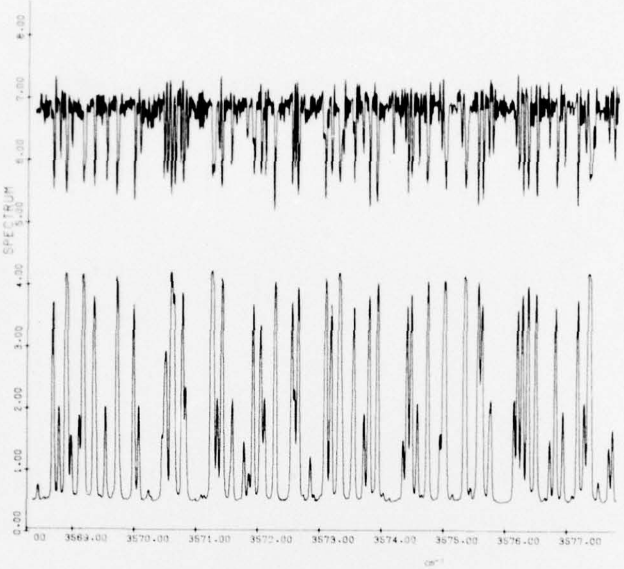

Figure 14. CO_2 Hot Cell Spectrum (upper curve) and Simulated Spectrum (lower curve), 3569 – 3577 cm^{-1}

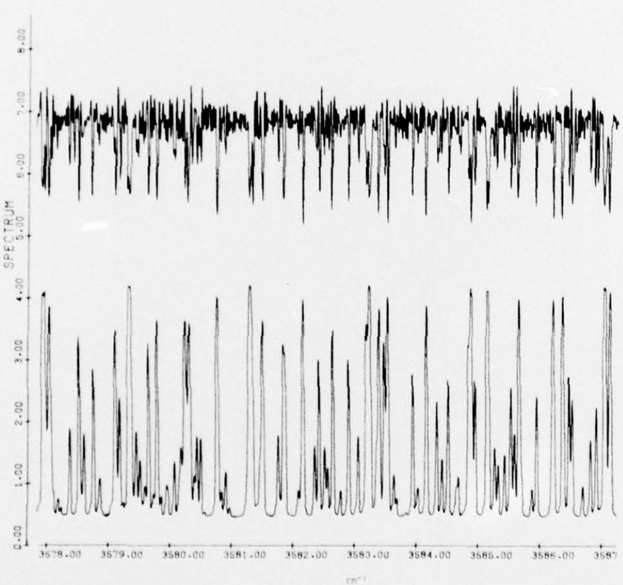

Figure 15. CO_2 Hot Cell Spectrum (upper curve) and Simulated Spectrum (lower curve), 3578 – 3587 cm^{-1}

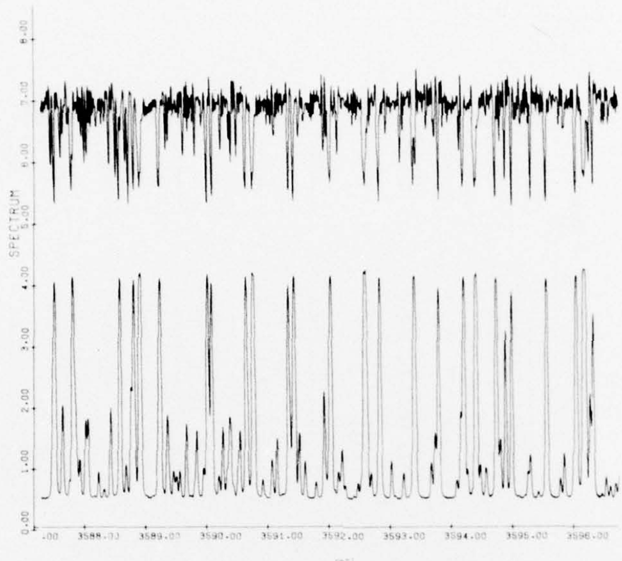

Figure 16. CO_2 Hot Cell Spectrum (upper curve) and Simulated Spectrum (lower curve), 3588 – 3596 cm^{-1}

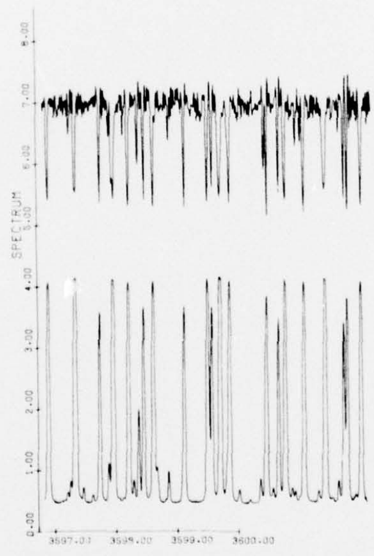

Figure 17. CO_2 Hot Cell Spectrum (upper curve), and Simulated Spectrum (lower curve), 3597 – 3600 cm^{-1}

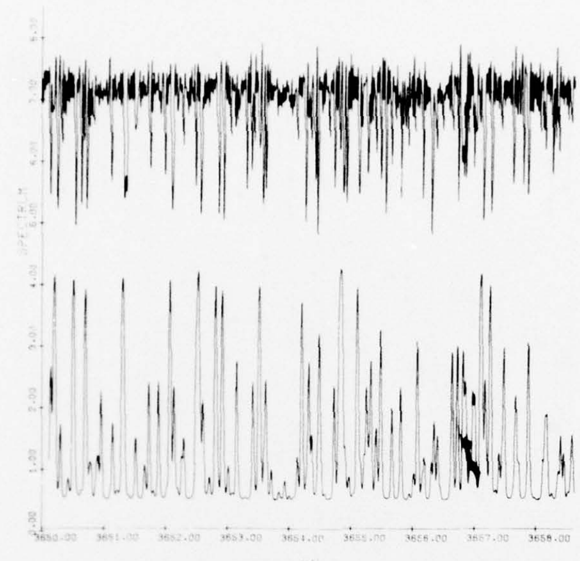

Figure 18. CO_2 Hot Cell Spectrum (upper curve) and Simulated Spectrum (lower curve), 3650 - 3658 cm^{-1}

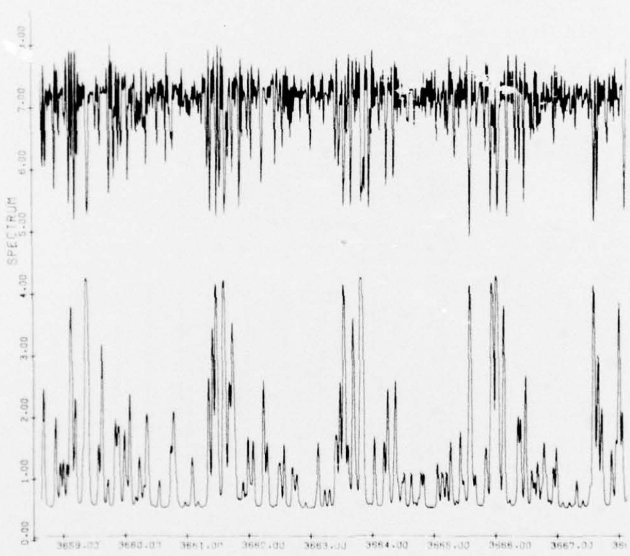

Figure 19. CO_2 Hot Cell Spectrum (upper curve) and Simulated Spectrum (lower curve), 3659 - 3667 cm^{-1}

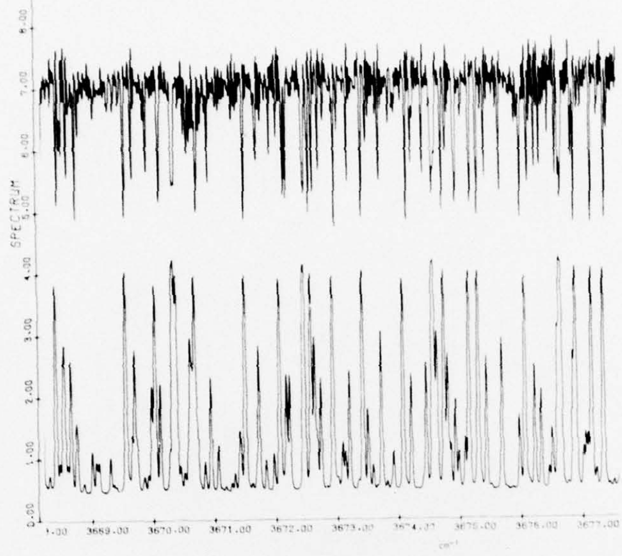

Figure 20. CO_2 Hot Cell Spectrum (upper curve) and Simulated Spectrum (lower curve), 3668 – 3677 cm^{-1}

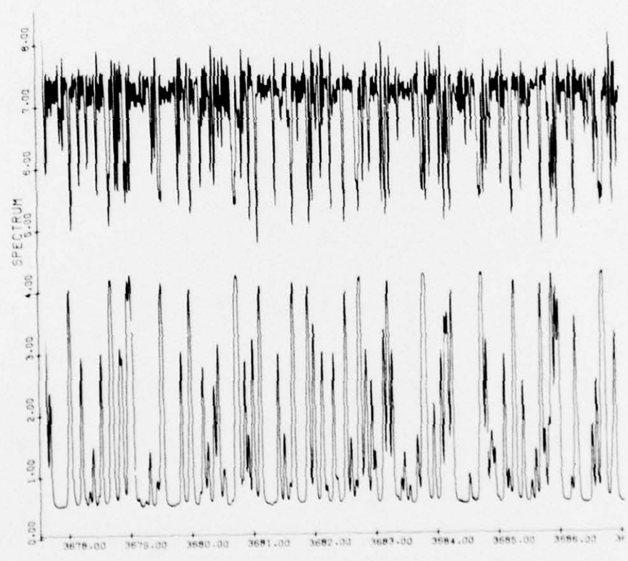

Figure 21. CO_2 Hot Cell Spectrum (upper curve) and Simulated Spectrum (lower curve), 3678 – 3686 cm^{-1}

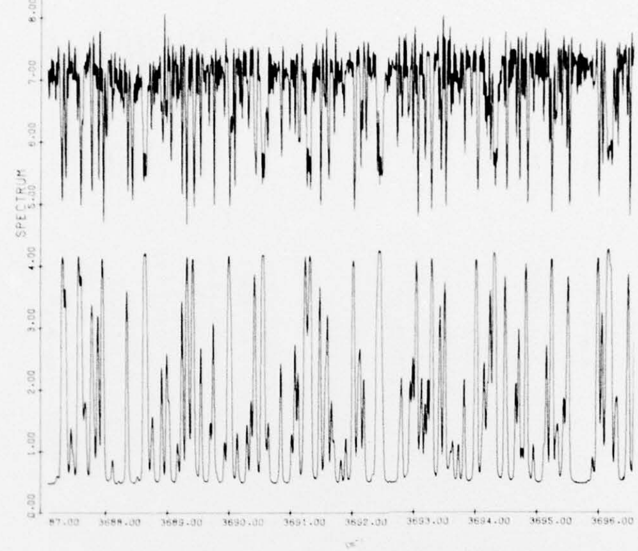

Figure 22. CO_2 Hot Cell Spectrum (upper curve) and Simulated Spectrum (lower curve), 3687 - 3696 cm^{-1}

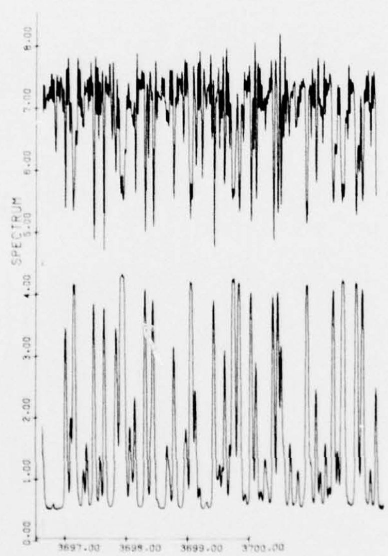

Figure 23. CO_2 Hot Cell Spectrum (upper curve) and Simulated Spectrum (lower curve), 3697 - 3700 cm^{-1}

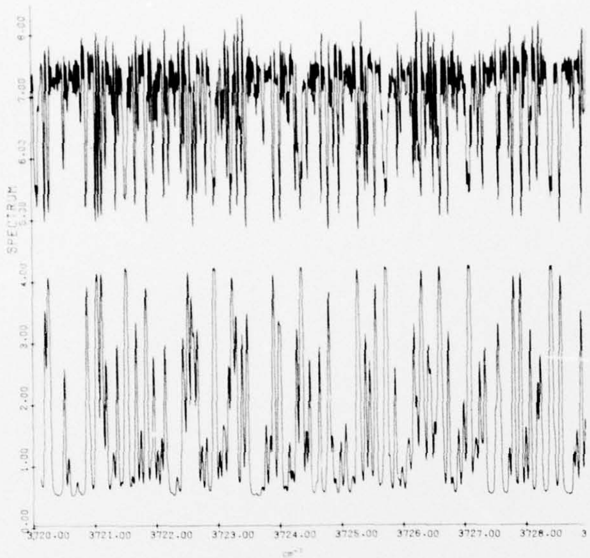

Figure 24. CO_2 Hot Cell Spectrum (upper curve) and Simulated Spectrum (lower curve), 3720 - 3728 cm^{-1}

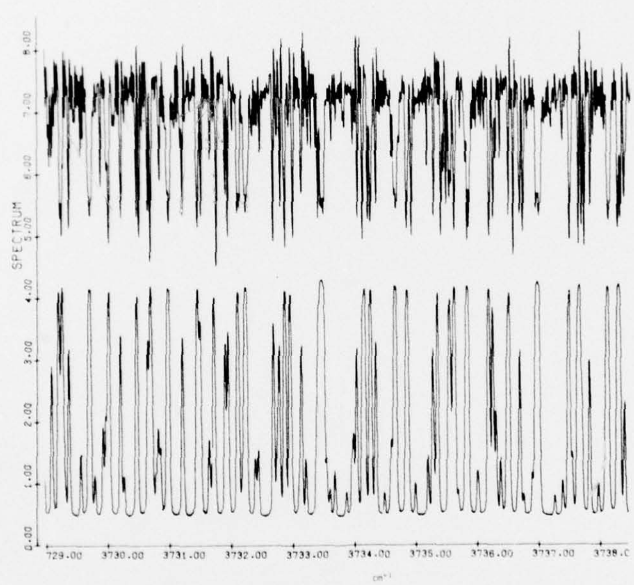

Figure 25. CO_2 Hot Cell Spectrum (upper curve) and Simulated Spectrum (lower curve), 3729 - 3738 cm^{-1}

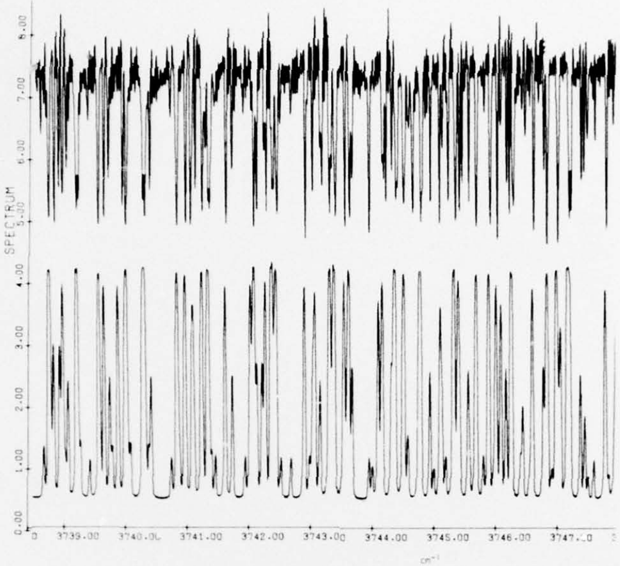

Figure 26. CO_2 Hot Cell Spectrum (upper curve) and Simulated Spectrum (lower curve), 3739 – 3747 cm^{-1}

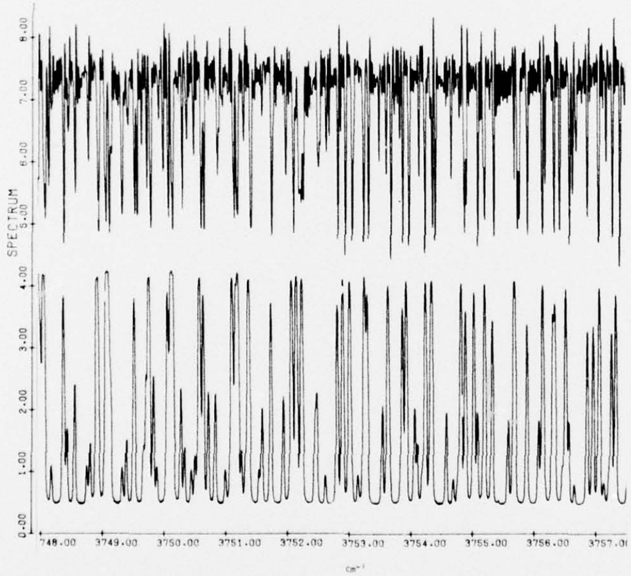

Figure 27. CO_2 Hot Cell Spectrum (upper curve) and Simulated Spectrum (lower curve), 3748 – 3757 cm^{-1}

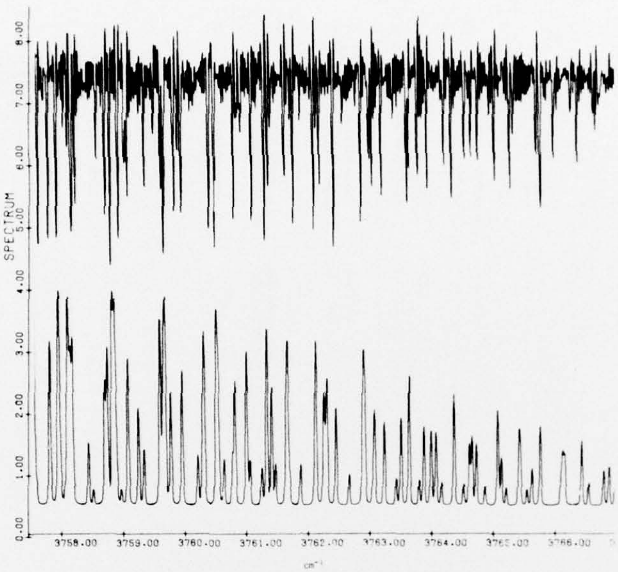

Figure 28. CO_2 Hot Cell Spectrum (upper curve) and Simulated Spectrum (lower curve), 3758 - 3766 cm^{-1}

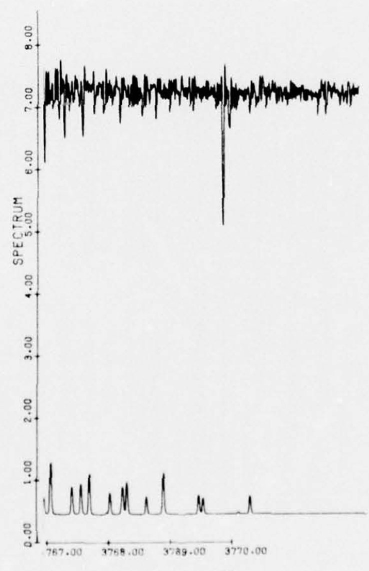

Figure 29. CO_2 Hot Cell Spectrum (upper curve) and Simulated Spectrum (lower curve), 3767 - 3770 cm^{-1}